applied sciences

MDPI

Article

Excitation and Relaxation Dynamics of the Photo-Perturbed Correlated Electron System 1*T*-TaS_2

Isabella Avigo [1], Ping Zhou [1], Matthias Kalläne [2], Kai Rossnagel [2], Uwe Bovensiepen [1] and Manuel Ligges [1,*]

[1] Fakultät für Physik, Universität Duisburg-Essen, 47048 Duisburg, Germany; isabella.avigo@uni-due.de (I.A.); ping.zhou@uni-due.de (P.Z.); uwe.bovensiepen@uni-due.de (U.B.)
[2] Institut für Experimentelle und Angewandte Physik, Christian-Albrechts-Universität zu Kiel, 24098 Kiel, Germany; kallaene@physik.uni-kiel.de (M.K.); rossnagel@physik.uni-kiel.de (K.R.)
* Correspondence: manuel.ligges@uni-due.de; Tel.: +49-203-379-4547

Received: 27 November 2018; Accepted: 20 December 2018; Published: 24 December 2018

Abstract: We investigate the perturbation and subsequent recovery of the correlated electronic ground state of the Mott insulator 1*T*-TaS_2 by means of femtosecond time-resolved photoemission spectroscopy in normal emission geometry. Upon an increase of near-infrared excitation strength, a considerable collapse of the occupied Hubbard band is observed, which reflects a quench of short-range correlations. It is furthermore found that these excitations are directly linked to the lifting of the periodic lattice distortion which provides the localization centers for the formation of the insulating Mott state. We discuss the observed dynamics in a localized real-space picture.

Keywords: non-equilibrium; mott-insulator; charge-density wave; photoemission

1. Introduction

Correlated electron systems play an important role in modern condensed matter physics, as they emerge in the context of e.g., high-temperature superconductivity [1] or metal-to-insulator transitions [2]. The equilibrium properties of such complex material are barely understood and very little is known about their non-equilibrium dynamics because the theoretical description of such strongly interacting many-body systems remains challenging [3]. Corresponding experiments in the time domain have been performed e.g., by investigating the re-emergence of charge order from a quenched disorder, induced by photo-perturbation, on the organic Mott insulator ET-F_2TCNQ, a system that only exhibits negligible electron-phonon interaction and, thus, can be well described by means of pure electronic models [4,5]. However, these dynamics might become more complex when the general case is addressed, namely, the investigation of systems where coupling to other degrees of freedom play an important role [6–8] and/or different types of order compete or coexist. In this letter, we discuss (i) the dynamics of a sudden quench of charge order, caused by femtosecond laser excitation, (ii) the subsequent recovery and (iii) the role of electron-phonon coupling in a Mott insulator that exhibits simultaneously strong electron-electron and electron-phonon interaction.

The layered transition metal dichalcogenide 1*T*-TaS_2 shows a variety of electronic and structural ordered phases [9,10]. In its high-temperature state, the system is metallic and can be characterized by a hexagonal arrangement of atoms within the Ta planes of the S-Ta-S building layers (Figure 1a). Cooling of the material gives rise to the formation of "David-star"-shaped polaron clusters, formed by 13 Ta-atoms, that leads to charge-density-wave (CDW) formation of different commensurability (Figure 1b–c), which can be described by sums of harmonics of both structures [11]. Below a critical temperature of 180 K, all clusters undergo a structural transition and a commensurate superstructure (c-CDW) is formed that is accompanied by a rearrangement of the partially filled Ta 5*d* band into

sub-manifolds, where the uppermost half-filled band is prone to a Mott-Hubbard transition, forming an occupied lower Hubbard band (LHB) and an unoccupied upper Hubbard band separated by a ∼400 meV band gap [12,13]. This formation of a charge density wave (long-range order) that coexists with a Mott-insulator phase (short-range correlations) [14] finally turns the system into an insulator. This well-established, but simplified picture of the in-plane properties is currently amended by experimental and theoretical work [15,16] of the out-of-plane properties that furthermore influence the electronic structure of the system.

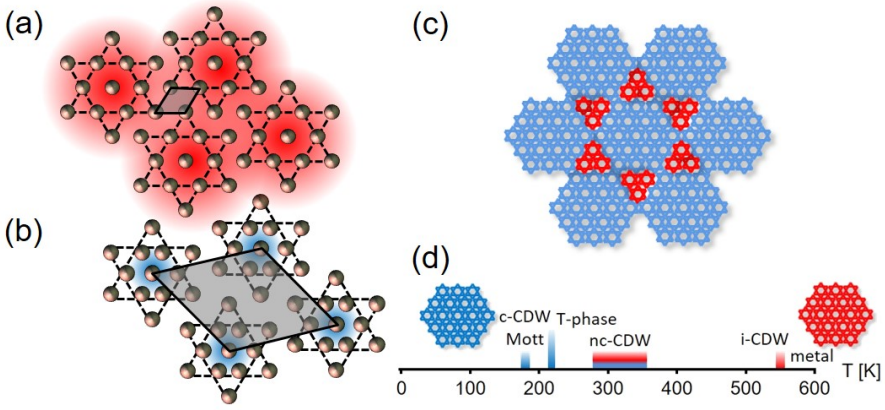

Figure 1. Local nuclear configuration in the Ta-plane of 1*T*-TaS_2 in the metallic high- and insulating low-temperature phase ((**a**,**b**), respectively); Grey shaded areas indicate the primitive 1×1 and $\sqrt{13} \times \sqrt{13}R13.9°$ superstructure unit cells. Upon contraction of the individual stars, the charge density (indicated as blue and red shaded areas) localizes on the central atom of the polaron cluster. At elevated temperatures, periodic arrangements of insulating and metallic domains are formed as depicted in (**c**); which shows the corner-sharing hexagon model of the nc-phase proposed from X-ray diffraction data [11], while edge-sharing hexagons were reported from transmission electron microscopy studies [17,18]; (**d**) Schematic overview of the different equilibrium phases, being either dominated by insulating (blue) or conducting (red) domains. (*c*-commensurate, *T*-triclinic, *nc*-nearly commensurate, *i*-incommensurate phase).

Femtosecond time-resolved experiments provided deep insight into this complex interplay between coexisting periodic lattice distortion and charge order, mainly by studying the photo-induced dynamics of the c-CDW/Mott phase. Upon optical excitation, ultrafast doublon dynamics are triggered [13] and the system can be driven into a "cross-over" phase [19–21] that exhibits an increased spectral weight at the Fermi level, accompanied by the excitation of a coherent optical phonon, identified as the CDW amplitude mode [19,20,22,23] and prompt collapse of charge order [19,23,24]. Recently, a hidden photo-induced state was reported that is unaccessible under equilibrium conditions [25–27] and is characterized by a specific mesoscopic real-space arrangement of polarons that can be driven on ultrafast time scales. Similar experimental results have been obtained by ultrafast electron diffraction, where ultrafast control of domain walls in the nearly commensurate nc-phase was reported upon intense optical excitation [28]. Furthermore, superconductivity (which arises at a critical temperature of T_c = 2 K) was associated with small amounts of disorder in the low-temperature c-CDW state of 1*T*-TaS_2 [29]. The distinct optical and electrical properties of the hidden state as well as those of the different equilibrium ground states highlight the importance of the nanoscale real-space structure and promises a way for ultrafast control of this correlated electron system.

Based on time-resolved photoemission we discuss the details of the photo-excitation mechanism generating quenched charge disorder, which amends our recent discussion of ultrafast doublon dynamics in 1*T*-TaS_2 [13]. We show that the corresponding dynamics are directly linked to a local lifting of CDW order. We propose in this work that the photo-induced dynamics can be discussed in a

localized picture and that re-equilibration of the system after optical perturbation occurs on the time scale of a few vibrational cycles of the charge-density amplitude mode.

2. Experiments and Results

Our femtosecond photoemission experiments were carried out in a pump-probe scheme in normal emission geometry on in situ cleaved single crystals of 1*T*-TaS_2 that were grown by a standard chemical vapor transport method (see [13] for details). The samples were cleaved in ultrahigh vacuum at room temperature. The obtained surfaces were excited with 50 fs laser pulses from a commercial regenerative Ti:Sa laser amplifier (Coherent RegA 9040, $\hbar\omega_1$ =1.55 eV) and subsequently probed by direct photoemission using UV pulses ($\hbar\omega_2$ =6.2 eV), which were generated by two consecutive frequency-doubling processes of the fundamental pulses using β-barium borate crystals. The overall temporal and spectral resolutions were 95 fs and 55 meV, respectively. Excitation fluences (given here as incident fluences F) increased up to the regime where switching of the samples into the hidden state could be expected ($F > 1$ mJ cm^{-2}) [25,27]. Time zero was determined with an accuracy better than 5 fs, similar to the method used in Ref. [13]. A typical dataset obtained in the c-CDW/Mott phase (T = 80 K, F =730 µJ cm^{-2}) is shown in Figure 2a as a false-color representation, which suitably visualizes the variety of effects observed upon optical excitation. Such data resemble previous studies under similar conditions [19,20,23,24] that revealed (i) a transient quench and subsequent recovery of the LHB signature at $E - E_F \approx -0.17$ eV, (ii) a partial filling of the formerly gapped spectral region around E_F, (iii) the generation of a hot carrier population continuum and (iv) oscillations of the spectral weight due to the coherent excitation of the CDW amplitude mode phonons with frequencies of 2.4 and 2.5 THz. A similar behavior is found for all excitation fluences used. Our discussion here will focus on the dynamics of the LHB and the signature of the amplitude mode of the commensurate CDW phase.

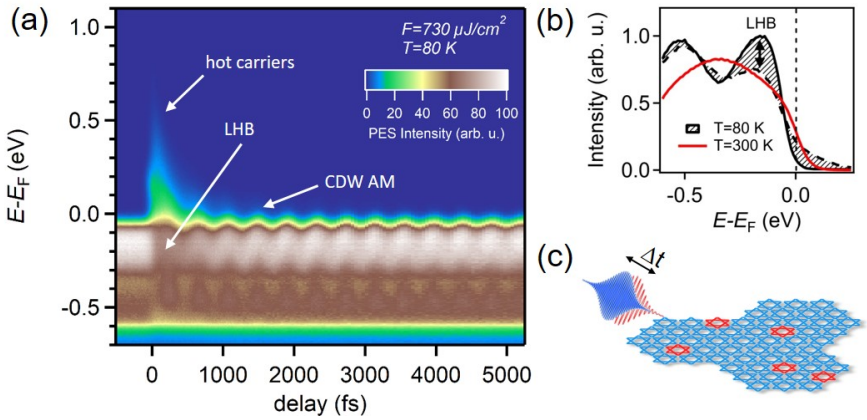

Figure 2. (**a**) False-color representation of data obtained for an incident pump fluence F = 730 µJ cm^{-2} at sample base temperature T = 80 K. An instantaneous collapse and subsequent recovery of the LHB signature is observed along with the generation of a hot carrier continuum and oscillations of the spectral weight due to the coherent excitation of the CDW amplitude mode; (**b**) Photoemission spectra of the room-temperature and insulating phase (red and black solid lines, respectively). The shaded area indicates the photo-induced change of the low-temperature spectrum upon strong optical pumping (F = 1700 µJ/cm^2); (**c**) Illustration of the laser-excited charge ordered state, as concluded from the femtosecond photoemission studies. The sample is excited by a femtosecond IR pulse to partly turn single polaron clusters (blue stars) to become metallic (red stars). Subsequent probing through photoemission by the UV pulse maps the coexistence of both phases at delay Δt.

A particular aspect we focus on is detailed in Figure 2b, which shows photoemission spectra before and after (Δt = +100 fs) laser excitation for the c-CDW/Mott phase in comparison with an equilibrium room-temperature spectrum. Upon optical excitation, a quench of the LHB signature is observed that

is accompanied by a partial filling of the formerly gapped spectral region ($E - E_F \approx -0.2 \ldots + 0.2$ eV), indicating that the Mott phase is (partially) molten and that the corresponding short-range correlations are quenched.

The shown spectra are recorded under similar conditions, which allows for a direct comparison of the excited c-CDW phase spectrum with the room-temperature equilibrium spectrum. Comparing the spectra, we find for the maximum achievable quench of the LHB that the spectra of the excited c-CDW phase and the equilibrium metallic phase become comparable in the energetic window of the LHB signature. While this potentially hints towards a complete quench of the short-range correlations, both spectra are still distinguishable and, thus, a transient state different from the room-temperature phase is observed. Figure 3a shows the maximum quench of the LHB spectral signature as a function of incident pump fluence, as extracted from the LHB dynamics (Figure 3b), where we analyzed the minimum value of the LHB intensity that can be found for all delay times. In agreement with [20], we find an almost linear dependence of the intensity loss from incident pump fluence for $F < 400$ μJ cm^{-2}. This indicates a perturbative excitation regime where the LHB intensity directly corresponds to the number of excited quasi-particles or the amount of deposited energy. For higher F, the observed quench saturates and a maximum suppression of approximately 25 percent is found, resulting in the finite spectral weight that corresponds to the one found in the room-temperature phase as mentioned above. We will discuss these two major findings, (i) a high intensity loss of the LHB signature and (ii) the saturation of this intensity loss as a function of incident fluence, in the following in more detail.

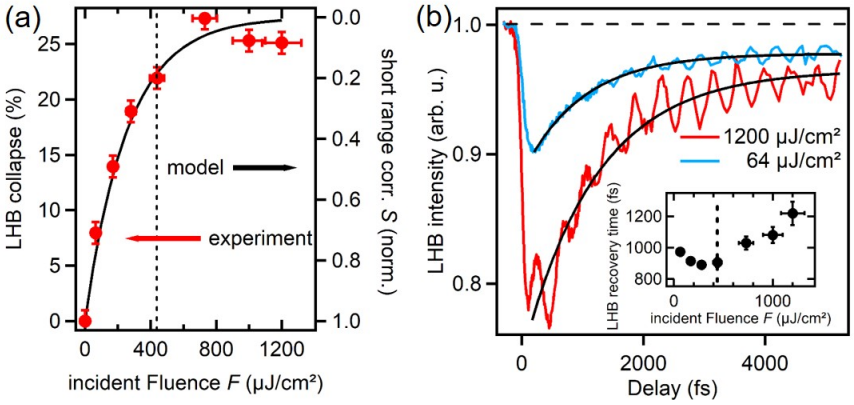

Figure 3. (**a**) Maximum collapse of the LHB peak intensity as a function of incident pump fluence, as extracted from the transient LHB intensity (**b**). The solid black line in (**a**) shows the result of the model calculation (see text) and the corresponding quench of short-range correlation S. The vertical dashed line indicates the fluence at which deviations from a linear dependence are found and the LHB collapse starts to saturate; (**b**) Time dependence of the LHB signature for two selected excitation fluences (F = 1200 μJ cm^{-2} and F = 64 μJ cm^{-2}). Solid lines are exponential fits used to extract the LHB recovery times (inset in (**b**)), neglecting the oscillatory part of the signal. The resulting error bars are shown in the inset. Please note that the saturation level at higher delays is below the value obtained before pumping (indicated by the dashed horizontal line).

In a simplified picture, the 13 Ta 5*d* valence electrons of each polaron cluster form sub-bands, where the uppermost half-filled band stemming from the 13th excess electron is prone to the Mott-Hubbard transition. A loss in LHB intensity reflects either a depopulation of the corresponding electronic band or transient changes in the electronic density of states caused by the suppression of on-site electron-electron interaction [30]. The rather high intensity loss of the LHB signature is likely incompatible with a simple depopulation scheme because it would imply that a majority of the valence electrons are excited, a situation that potentially destabilizes the crystal. Furthermore, no comparable intensity losses are observed in other energetic regions accessible in the experiment. We rather interpret the LHB spectral signature intensity as a direct measure of the strength of short-range electron

correlation S in the system that can be understood as an "order parameter" for the charge ordered state, which is also reflected in temperature-dependent equilibrium photoemission data [12]. We therefore conclude that the saturation of this loss reflects the complete collapse of the short-range interaction responsible for the emergence of the Mott gap and the LHB signature.

In accordance with the nanoscale coexistence of insulating and metallic domains (Figure 1), we discuss the transient quench of electronic correlations in a real-space picture. First we note that the geometrical cluster density $n_0 = 7 \times 10^{13}$ cm^{-2} [31] is somewhat smaller than the number of incident pump photons $\frac{F}{\hbar\omega_1} \approx 1.6 \times 10^{15}$ cm^{-2} for $F = 400$ μJ cm^{-2} at the approximate saturation threshold, which implies that the excitation of all polaron clusters is in principle possible. Under the assumption of a linear response to the pump laser pulse, where every absorbed photon can excite a single cluster site once, the excited cluster density n_x as a function of incident pump fluence F can be described by a simple differential equation of the form

$$\frac{dn_x}{dF} = \frac{\gamma}{\hbar\omega_1}\left(\frac{n_0 - n_x}{n_0}\right), \tag{1}$$

where $\gamma = (1 - R)(1 - e^{-c/\lambda})$ is the pump photon absorption probability within the probed sample depth c, which we assume to be the first sample layer (c = 0.596 nm [31]). R = 0.49 and λ = 70 nm are the optical reflectivity and penetration depth for $\hbar\omega_1$ = 1.55 eV, respectively [21,32]. Assuming a linear relation between the number of excited clusters and the LHB intensity, the intensity collapse is given by $C = n_x/n_0$. As mentioned before, the saturation of the LHB intensity loss results in a finite spectral weight in the corresponding energy window which is comparable to the one found in the room-temperature phase. Correspondingly, the correlation strength S might be defined as S = 1 in the unperturbed state and S = 0 in the case where the LHB intensity is completely lost and the 25 percent reduction in intensity is observed ($S \propto (1 - C)$).

The solution of Equation (1) is shown as a solid line in Figure 3a. Despite the simplicity of the model and the underlying assumptions, both, the almost linear dependence for F < 400 μJ cm^{-2} and the saturating behavior for F > 400 μJ cm^{-2} can be reproduced without further rescaling. For high excitation fluences (F > 1000 μJ cm^{-2}), an almost complete reduction of short-range correlation is observed. As mentioned before the excitation fluences under which an almost complete quench occurs are close to those for switching the material into the hidden phase.

Based on the above discussions, we will now turn towards the re-equilibration of the system, which is reflected by the recovery of LHB intensity (Figure 3b). The recovery of the LHB intensity is shown in Figure 3b for two different pump fluences. The recovery times τ_{LHB} (inset in Figure 3b) are extracted from the transients of the LHB intensity by fitting with an exponential function that was convoluted with a Gaussian resolution function (solid lines in Figure 3b). For low excitation densities (F < 400 μJ cm^{-2}), the recovery times slightly decrease as function of F from 1 ps to 900 fs with a minimum occurring at the excitation level where the saturation of the LHB intensity quench sets in. For higher fluences, the recovery time increases up to a maximum value of 1.2 ps, which corresponds to a few oscillation cycles of the CDW amplitude mode (T_{CDW} = 400 fs). In general, these timescales are significantly longer than the carrier hopping time $t = \hbar/W \approx 14$ fs [13,19] or the characteristic electron-phonon energy transfer time of $\tau_{e-ph} \approx$ 200–350 fs reported in literature [20,33]. This difference in time scales raises the question on the nature of the complete recovery of the Mott state, which we address here.

As on the sub-picosecond timescale a majority of the electronic excess energy is already transferred to the lattice system via incoherent excitation of phonons, it is reasonable to first discuss the scenario of an almost thermalized, heated lattice during the recovery of charge order. Assuming that the total excess energy provided by the pump pulse is transferred to the lattice system, we calculated a final lattice temperature of 104 K for F = 1500 μJ/cm^2 and sample base temperature of 80 K, respectively [34]. Since the recovery time of the LHB signature is only weakly and non-monotonously dependent of excitation fluence, a simple thermally activated process can clearly be excluded. As evident

from Figure 3b, the LHB intensity only partly recovers at longer delays (Δt = 5 ps) because the quasi-equilibrated state after a few ps is different from the state before excitation, since a finite amount of energy was deposited in the system. Similar reduction of the LHB intensity can also be found from temperature-dependent photoemission data recorded under equilibrium conditions [12]. The dynamic pathway between the initial and the quasi-equilibrated state can; however, not be explained by pure thermal effects as the LHB recovery ($\tau_{LHB} \approx 1$ ps) does not occur on the electron-phonon energy transfer time scale ($\tau_{ephB} \approx$ 200–350 fs). In fact, the recovery occurs slower than any other process observed in our experiment which implies that either non-local relaxation phenomena (mapped via **k**-dependent studies not performed here) or non-thermalized states in the lattice system are responsible for the slow re-equilibration of the electronic subsystem. In fact, such long-living non-equilibrium situations in the lattice system have been reported earlier [35] and are also present here.

As can be seen from the data in Figure 2a, the excitation of the CDW amplitude mode results in spectral shifts of the photoemission spectra that that can be analyzed best in the vicinity of the Fermi level E_F, where the photoemission intensity abruptly changes as a function of energy. Figure 4a shows the integrated photoemission intensity in this spectral range ($E - E_F = -65$ ... -45 meV) for several pump fluences. Long-living oscillations with damping times of the order of 10–20 ps are found and the photonic subsystem is still in a non-equilibrium situation after the majority of electronic energy is transferred to the lattice. Since these damping times are substantially longer than the recovery times of the LHB signature, the population of the amplitude mode phonon does not limit but potentially drives the electronic re-equilibration of the system. The amplitude of the observed oscillations, as extracted from the transients in Figure 4a, shows a similar saturating behavior as the LHB quench (Figure 4b), indicating that the local excitation of polaron clusters and the CDW amplitude mode oscillations are inherently linked.

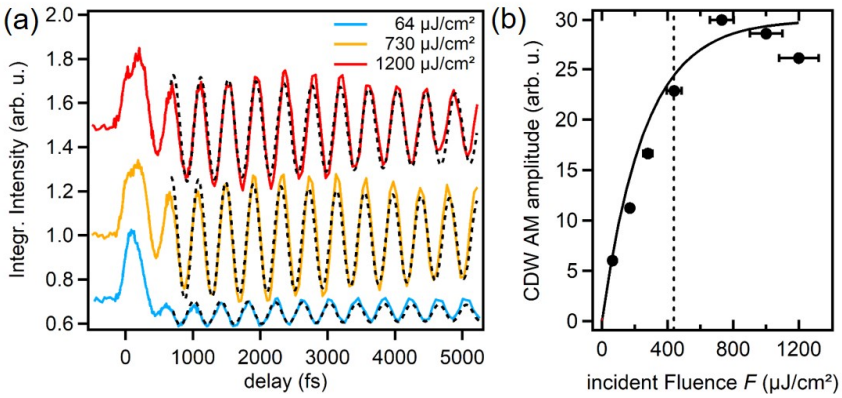

Figure 4. (**a**) Transient spectral intensity in a small energy window ($E - E_F = -65$ ... -45 meV) from which the CDW amplitude mode dynamics can be extracted. Dashed lines are fits to the data, assuming a damped single oscillatory component $I(t) = A \cdot exp(-t/\tau) \cdot cos(\omega t + \varphi) + B$ with a frequency of 2.5 THz. Typical goodness of fits are χ^2 =0.15-0.16; (**b**) shows the amplitude A of the oscillation as a function of fluence. The solid black line is the result of the modelling already shown in Figure 3a. Vertical dashed lines indicate the fluence range in which saturation occurs.

3. Discussion

The non-equilibrium dynamics observed here are significantly different from those observed in, e.g., simple metals. In such systems, optical excitation generates a non-equilibrium distribution of electrons which thermalizes on the 10–100 fs timescale [36–39]. The resulting high-temperature distribution function subsequently relaxes on the few ps timescale due to electron-phonon interaction [40–42], leaving the system behind in a new equilibrated state that can be characterized by one uniform, transient temperature. Here, we observe a persisting non-equilibrium situation in the electronic subsystem on the ps timescale (Figure 3b), when a majority of electronic excess energy is

already transferred to the lattice [20,33]. A particular finding is that the recovery of this non-equilibrium state is only partial, as the LHB intensity is not fully restored after several ps. Similar persisting, transient states were also observed during the structural response of photo-excited 1*T*-TaS_2 [35], where the formation of a long-living (>10 ps), quasi-equilibrated lattice state was found to occur on timescales comparable to the LHB recovery times discussed here. Our data clearly show a link between the CDW periodic lattice distortion and short-range electronic correlations, as both signatures show the same saturating behavior, see Figures 3a and 4b.

From our experimental findings we conclude on a hierarchy of time scales that we discuss in a localized picture:

(i) The optical excitation of the electronic subsystem results in a prompt collapse of the Mott state [24] which is reflected by a transient reduction of the LHB intensity. In a simplified scheme, these localized excitations of ground state carriers result in the generation of spatially randomly distributed "metallic" clusters which are similar to the discommensurations found in the higher temperature phases and are reflected by a partial filling of the formerly gapped spectral region around E_F. This situation is not stable as evident from the different ordered equilibrium structures that exhibit well-defined long-range configurations of the lattice. These clusters can be interpreted as defects of the CDW and locally trigger the excitation of the CDW amplitude mode phonon. We assume the excitation of the CDW amplitude mode phonon to be local, e.g., on single clusters. This assumption is justified, as the corresponding optical phonon branches are of narrow band width [43,44], which allows for our experimentally observed dephasing times of >10 ps (Figure 4a). On these ultrashort time scales (<100 fs), a majority of excess energy is stored in the electronic subsystem.

(ii) The electronic excess energy is largely transferred to the lattice system within few 100 fs due to the incoherent excitation of phonons. While the electronic system is almost thermalized [20], the lattice system is in a non-equilibrium state as the CDW amplitude phonon mode is still highly populated.

(iii) The LHB signature recovers due to the reformation of the Mott state on the 1 ps time scale. The final, quasi-equilibrated state after a few ps is different from the initial state as evident from partial recovery of LHB intensity (Figure 3b) and characterized by an decreased amplitude of the CDW lattice distortion [35] that persists up to the time scale of 10 ps, where the CDW amplitude mode phonon is largely damped out due to anharmonic coupling.

(iv) Full re-equilibration of the system due to heat transfer out of the excited sample volume on nano- to microsecond time scales occurs, resulting in a reduction of excited clusters within the probed sample volume [28]. This process leads to a re-establishment of the initial (mesoscopic) state before excitation, unless the system has been switched into a meta-stable, hidden state [25] due to sufficiently strong excitation.

Of particular interest here is the dynamic pathway between the initial state after excitation (i) and the final state achieved after few ps (iii), as it is discussed in the context of the formation of the hidden state [25–27] and domain wall dynamics [28]. Based on the localized excitation scheme and our experimental findings we propose the following scenario:

The quasi-equilibrated state (iii) after photo-excitation must be characterized by specific real-space arrangements of the excited clusters, as randomly distributed defects tend to aggregate to form domain walls which can effectively lower the free energy of the system [45]. Correspondingly the equilibration of the initial excited state (i) requires hopping of the excited polarons. Due to the weak and non-monotonous dependence of the LHB recovery time on excitation fluence (Figure 3b), we exclude thermally activated processes to be responsible for this spatial rearrangement.

Readopting the equilibrium pictures of CDW/Mott-formation in 1*T*-TaS_2 (Figure 1), we expect that the contraction of individual polaron clusters leads to the formation of localization centers of the charge density. Accordingly, inter-star charge transfer caused by de-localization of the ground state carriers requires expansion of the clusters and, thus, a nuclear configuration that is facilitated by the population of the CDW amplitude mode phonon which remains populated on the 10 ps time scale (Figure 4a). This transfer of excitation should not be confused with the significantly faster hopping of

carriers in the Mott ground state [13], since it also requires a transfer of the lattice excitation which leads to an effective reduction of the systems free energy. Finally, full equilibration of the system occurs on timescales of a few oscillation periods, which allows for the formation of the final real-space configuration. This sequence is sketched in Figure 5.

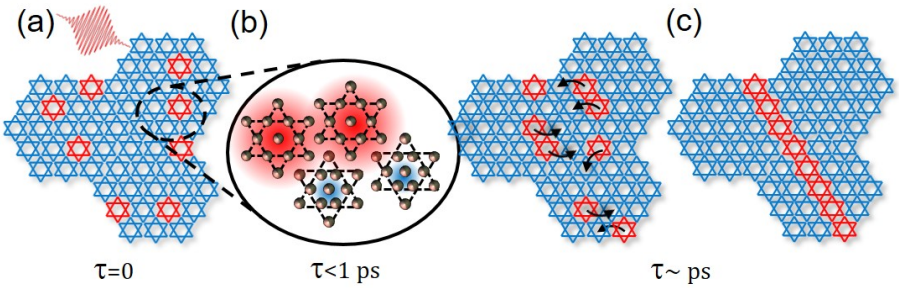

Figure 5. Proposed sequence of photo-induced dynamics. Prior to optical excitation, the structure is governed by insulating domains (blue). Optical excitation leads to randomly distributed excited (red) clusters (**a**) that act as defects for the CDW; On a timescale less than 1 ps, a majority of electronic excess energy is transferred to the lattice and the CDW amplitude mode phonon is highly populated, allowing for local hopping of the electronic excitations (**b**); After a few picoseconds, a new real-space structure is formed and the system reached its new quasi-equilibrium state (**c**).

The real-space picture discussed here is compatible with all experimental findings. The formation of the correlated electronic ground state is inherently linked to the periodic lattice distortion, which is reflected by the saturating behavior of both corresponding signatures (Figures 3a and 4b). The optical quench of charge order coherently excites the associated optical phonon modes, which—on the other hand—facilitates charge transfer processes between individual clusters. On long time scales, the system is left behind with a finite amount of deposited energy which leads to an increase in electronic and lattice temperature, reflecting either a new real-space configuration that can also be found under equilibrium conditions or exotic states otherwise not accessible. The details of this newly formed state will critically depend on the excitation conditions [25], finite defect density [13] or chemical doping level [26] and energy contributions from domain wall interactions [45,46], allowing for a large parameter space to tune the macroscopic properties of this material on ultrafast time scales.

4. Conclusions

In summary, the quench and recovery of charge order in the combined CDW/Mott system 1*T*-TaS_2 can be discussed in a real-space picture rather than in momentum space. Optical excitation leads to a spatially random distribution of excited polaron clusters that subsequently relax by spatial rearrangement, forming a new real-space configuration of insulating and conducting domains. This rearrangement is facilitated by the coherent excitation of the CDW amplitude mode, which allows for local inter-star charge transfer and rearrangement of domains on mesoscopic length scales.

Author Contributions: Conceptualization, M.L. and U.B.; Validation, I.A., M.L. and U.B.; Formal Analysis, I.A. and M.L.; Investigation, I.A.; Resources, P.Z., M.K. and K.R.; Writing—Original Draft Preparation, M.L.; Writing—Review & Editing, I.A., M.L., U.B. and K.R.; Funding Acquisition, M.L. and U.B.

Funding: This work was funded by the Deutsche Forschungsgemeinschaft (DFG, German Research Foundation)—Projektnummer 278162697—SFB 1242.

Acknowledgments: We thank Kerstin Hanff for technical support (sample administration) and Klaus Sokolowski-Tinten for fruitful discussion.

Conflicts of Interest: The authors declare no conflict of interest.

Abbreviations

The following abbreviations are used in this manuscript:

CDW	Charge Density Wave
c-CDW	Commensurate Charge Density Wave
LHB	Lower Hubbard Band

References

1. Plakida, N. *High-Temperature Cuprate Superconductors*; Springer Series in Solid-State Sciences; Springer: Berlin/Heidelberg, Germany, 2010; Volume 166.
2. Imada, M. Metal-insulator transitions. *Rev. Mod. Phys.* **1998**, *70*, 1039. [CrossRef]
3. Aoki, H. Nonequilibrium dynamical mean-field theory and its applications. *Rev. Mod. Phys.* **2014**, *86*, 779. [CrossRef]
4. Wall, S. Quantum interference between charge excitation paths in a solid-state Mott insulator. *Nat. Phys.* **2011**, *7*, 114–118. [CrossRef]
5. Mitrano, M. Pressure dependent relaxation in the photo-excited Mott insulator ET-F_2TCNQ: Influence of hopping and correlations on quasiparticle recombination rates. *Phys. Rev. Lett.* **2014**, *112*, 117801. [CrossRef] [PubMed]
6. Shen, W. Nonequilibrium melting of a charge density wave insulator via an ultrafast laser pulse. *Phys. Rev. Lett.* **2014**, *112*, 176404. [CrossRef] [PubMed]
7. Eckstein, M. Photoinduced States in a Mott Insulator. *Phys. Rev. Lett.* **2013**, *110*, 126401. [CrossRef] [PubMed]
8. Eckstein, M. Dielectric breakdown of Mott insulators—doublon production and doublon heating. *J. Phys. Conf. Ser.* **2013**, *427*, 012005. [CrossRef]
9. Wilson, J.A. Charge-density waves and superlattices in the metallic layered transition metal dichalcogenides. *Adv. Phys.* **1975**, *24*, 117–201. [CrossRef]
10. Sipos, B. From Mott state to superconductivity in 1*T*-TaS_2. *Nat. Mater.* **2008**, *7*, 960–965. [CrossRef] [PubMed]
11. Spijkerman, A. X-ray crystal-structure refinement of the nearly commensurate phase of 1*T*-TaS_2 in (3+2)-dimensional superspace. *Phys. Rev. B* **1997**, *56*, 13757. [CrossRef]
12. Dardel, B. Spectroscopic signatures of phase transitions in a charge-density-wave system: 1*T*-TaS_2. *Phys. Rev. B* **1992**, *46*, 7407–7412. [CrossRef]
13. Ligges, M. Ultrafast doublon dynamics in 1*T*-TaS_2. *Phys. Rev. Lett.* **2018**, *120*, 166401. [CrossRef] [PubMed]
14. Fazekas, P. Electrical, structural and magnetic properties of pure and doped 1*T*-TaS_2. *Philos. Mag. B* **1979**, *39*, 229–244. [CrossRef]
15. Ngankeu, A. Quasi-one-dimensional metallic band dispersion in the commensurate charge density wave of 1*T*-TaS_2. *Phys. Rev. B* **2017**, *96*, 195147. [CrossRef]
16. Ritschel, T. Orbital textures and charge density waves in transition metal dichalcogenides. *Nat. Phys.* **2015**, *11*, 328–331. [CrossRef]
17. Ishiguro, T. Electron microscopy of phase transformations in 1*T*-TaS_2. *Phys. Rev. B* **1991**, *44*, 2046–2060. [CrossRef]
18. Ishiguro, T. High-resolution electron microscopy of discommensuration in the nearly commensurate phase on warming of 1*T*-TaS_2. *Phys. Rev. B* **1994**, *52*, 759–765. [CrossRef]
19. Perfetti, L. Time Evolution of the Electronic Structure of 1*T*-TaS_2 through the Insulator-Metal Transition. *Phys. Rev. Lett.* **2006**, *97*, 067402. [CrossRef]
20. Perfetti, L. Femtosecond dynamics of electronic states in the Mott insulator 1T-TaS2 by time resolved photoelectron spectroscopy. *New J. Phys.* **2008**, *10*, 053019. [CrossRef]
21. Dean, N. Polaronic Conductivity in the Photoinduced Phase of 1*T*-TaS_2. *Phys. Rev. Lett.* **2011**, *106*, 016401. [CrossRef]
22. Demsar, J. Femtosecond snapshots of gap-forming charge-density-wave correlations in quasi-two- dimensional dichalcogenides 1*T*-TaS_2 and 2*H*-$TaSe_2$. *Phys. Rev. B* **2002**, *66*, 041101. [CrossRef]
23. Hellmann, S. Time-domain classification of charge-density-wave insulators. *Nat. Commun.* **2012**, *3*, 999. [CrossRef] [PubMed]

24. Petersen, J.C. Clocking the Melting Transition of Charge and Lattice Order in 1*T*-TaS_2 with Ultrafast Extreme-Ultraviolet Angle-Resolved Photoemission Spectroscopy. *Phys. Rev. Lett.* **2011**, *107*, 177402. [CrossRef] [PubMed]
25. Stojchevska, L. Ultrafast switching to a stable hidden quantum state in an electronic crystal. *Science* **2014**, *11*, 177–180. [CrossRef] [PubMed]
26. Stojchevska, L. Stability of the light-induced hidden charge density wave state within the phase diagram of $1T - TaS_{2-x}Se_x$. *Phys. Rev. B* **2018**, *98*, 195121. [CrossRef]
27. Avigo, I. Accessing and probing of the photoinduced hidden state in 1*T*-TaS_2 with time- and angle-resolved photoemission spectroscopy. *Proc. SPIE Spintronics IX* **2016**, *9931*, 99313V. [CrossRef]
28. Zong, A. Ultrafast manipulation of mirror domain walls in a charge density wave. *Sci. Adv.* **2018**, *4*, eaau5501. [CrossRef]
29. Xu, P. Superconducting phase in the layered dichalcogenide 1*T*-TaS_2 upon inhibition of the metal-insulator transition. *Phys. Rev. B* **2010**, *81*, 172503. [CrossRef]
30. Sohrt, C. How fast can a Peierls-Mott insulator be melted? *Faraday Discuss.* **2014**, *171*, 243–257. [CrossRef]
31. Yamamoto, A. Hexagonal domainlike structure in 1*T*-TaS_2. *Phys. Rev. B* **1983**, *27*, 7823. [CrossRef]
32. Mann, A. Probing the coupling between a doublon excitation and the charge-density wave in TaS_2 by ultrafast optical spectroscopy. *Phys. Rev. B* **2016**, *94*, 115122. [CrossRef]
33. Eichberger, M. Snapshots of cooperative atomic motions in the optical suppression of charge density waves. *Nature* **2010**, *468*, 799–802. [CrossRef] [PubMed]
34. Benda, J.A. Optical, electrical-transport, and heat-capacity studies of the solid solutions $Ti_xTa_{1-x}S_2$, $Zr_xTa_{1-x}S_2$, and $Ti_xNb_{1-x}Se_2$. *Phys. Rev. B* **1974**, *10*, 1409. [CrossRef]
35. Laulhé, C. X-ray study of femtosecond structural dynamics in the 2D charge density wave compound 1*T*-TaS_2. *Physica B* **2015**, *460*, 100–104. [CrossRef]
36. Fann, W. Direct measurement of nonequilibrium electron-energy distributions in subpicosecond laser-heated gold films. *Phys. Rev. Lett.* **1992**, *68*, 2834. [CrossRef] [PubMed]
37. Fann, W. Ultra-fast dynamics of electron thermalization, cooling and transport effects in Ru(001). *Appl. Phys. A* **2004**, *78*, 165–176.
38. Nicholson, C. Ultrafast Spin Density Wave Transition in Chromium Governed by Thermalized Electron Gas. *Phys. Rev. Lett.* **2016**, *117*, 136801. [CrossRef]
39. Gierz, I. Tracking Primary Thermalization Events in Graphene with Photoemission at Extreme Time Scales. *Phys. Rev. Lett.* **2015**, *115*, 086803. [CrossRef]
40. Brorson, S.D. Femtosecond Room-Temperature Measurement of the Electron-Phonon Coupling constant λ in Metallic Superconducters. *Phys. Rev. Lett.* **1990**, *64*, 2172–2175. [CrossRef]
41. Ligges, M. Observation of ultrafast lattice heating using time resolved electron diffraction. *Appl. Phys. Lett.* **2009**, *94*, 101910. [CrossRef]
42. Hohlfeld, J. Electron and lattice dynamics following optical excitation of metals. *Chem. Phys.* **2000**, *251*, 237–258. [CrossRef]
43. Benedek, G. Strong coupling of Rayleigh phonons to charge density waves in 1*T*-TaS_2. *Surf. Sci.* **1994**, *304*, 185–190. [CrossRef]
44. Sugai, S. Lattice Vibrations in the Charge-Density-Wave States of Layered Transition Metal Dichalcogenides. *Phys. Stat. Sol. B* **1985**, *129*, 13–39. [CrossRef]
45. Nakanishi, K. Domain-like Incommensurate Charge-Density-Wave States and the First-Order Incommensurate-Commensurate Transition in Layered Tantalum Dichalcogenides. *J. Phys. Soc. Jpn.* **1977**, *43*, 1839–1847. [CrossRef]
46. Bak, P. Commensurate phases, incommensurate phases and the devil's staircase. *Rep. Prog. Phys.* **1982**, *45*, 587. [CrossRef]